

HAAR WAVELET COLLOCATION METHOD FOR TELEGRAPH EQUATIONS WITH DIFFERENT BOUNDARY CONDITIONS

SHAHID AHMED ⁽¹⁾ SHAH JAHAN⁽²⁾ AND K.S NISAR ⁽³⁾

ABSTRACT. In this article, we study the Haar wavelet operational matrix approach for finding the numerical solutions of hyperbolic telegraph equations under suitable initial and boundary conditions. It has been approximated in both space and time using the Haar wavelets series with unknown coefficients. The advantage of the method is that it reduces the original problems to a set of algebraic equations that can be solved using standard methods. The precision and efficacy of the numerical method are shown via numerical examples. It has been shown experimentally that the approach is straightforward, precise, when compared to some of the current numerical methods.

1. INTRODUCTION

In 1957, Kirchoff was the first who introduce the telegraph equation for analyzing the disturbances inside objects and wave propagation. The general form of the hyperbolic telegraph equation is:

$$(1.1) \quad \frac{\partial^2 \rho(z, t)}{\partial t^2} + 2a \frac{\partial \rho(z, t)}{\partial t} + b^2 \rho(z, t) = \frac{\partial^2 \rho(z, t)}{\partial z^2} + R(z, t), \quad 0 \leq z \leq 1, \quad t \geq 0,$$

with initial conditions (ICs)

$$\rho(z, 0) = f(z), \quad \frac{\partial \rho(z, 0)}{\partial t} = f_1(z), \quad 0 \leq z \leq 1.$$

2020 *Mathematics Subject Classification.* 42C40; 65M99; 65T60; 35L10.

Key words and phrases. Collocation point, Dirichlet boundary condition, Haar wavelet, Neuman boundary conditions, Operational matrices, Telegraph equations.

Copyright © Deanship of Research and Graduate Studies, Yarmouk University, Irbid, Jordan.

Received: Jan. 2, 2023

Accepted: xxxxxxxxxxxx .

Dirichlet boundary conditions(DBCs)

$$\rho(0, t) = \Theta_0(t), \quad \rho(1, t) = \Theta_1(t), \quad 0 \leq t \leq 1,$$

and Neuman boundary conditions(NBCs)

$$\frac{\partial \rho(0, t)}{\partial z} = \Theta_0(z), \quad \frac{\partial \rho(z, 0)}{\partial t} = \Theta_1(z).$$

Where a and b are arbitrary constant, and $R(z, t)$ gives the field variable. Many physical and biological problems such as electric signals on transmission lines, pulsed blood flow inside the arteries, dispersive wave propagation, and random insect motions along hedge can be governed by the telegraph equation [14, 19, 27]. Over a couple of decades, the equation (1.1) has been solved by various analytical and numerical methods, such as Laplace transform method [2], DRBIE method [7] finite-difference method [4], homotopy perturbation method [28], cubic B-spline method [21], Adomain decomposition method [1], Monte-Carlo method [3], and Legendre Multiwavelet Galerkin method [30], reduced differential transform method [22], variational iteration method [5, 20], multi-wavelet Galerkin method [21]. It is frequently quite challenging to obtain an analytical solution to the partial differential equations (PDEs) that are accustomed to describe numerous physical and biological events, numerical approaches play an essential role in the process of finding solutions to these types of problems. The numerical techniques that are based on wavelets are one of the persuasive alternatives to the existing numerical methods. Wavelet methods achieved a great success in numerical analysis and approximation theory due to computational simplicity, straightforward methodology, and speedy convergence [16, 17, 29]. The most frequently adapted wavelets for solving differential equations include Legendre wavelets, Bernoulli wavelets, ultraspherical wavelets, and Haar wavelets. The differential equations solving wavelet methods are based on Galerkin techniques or the collocation approach. The Haar wavelet-based collocation techniques are mostly utilized for solving linear and nonlinear PDEs [17]. Other distinguishing features of these wavelets include their ability to detect the singular points, contain various boundary conditions, and can be integrated at arbitrary times. Since derivatives don't persist at partition locations, It is not feasible to directly solve PDEs with these wavelets, which is the biggest limitation. There are two different approaches that can be taken

to get out of this predicament. Interpolating splines are used to impose some order on the Haar wavelets is one approach, as proposed by Cattani. Another technique is to employ the Integral techniques, which were first presented by Chen and Hsiao [6]. They discussed the integration operational matrices for the Haar wavelet family. Lipik [15], established the Haar wavelet method to solve an ordinary and PDEs. Hussain et al. [11] studied the solution of proportional-delay Riccati differential equations using Haar Wavelet. Islam et al. [26] used wavelet collocation technique to solve boundary value problem, and also solved the elliptic boundary value problem by using Haar wavelet collocation technique. Hariharan and Kannan[9] solved some linear and nonlinear wave-type problems using Haar wavelet. For stability analysis for Haar wavelet collocation method one can see [6, 16, 17, 25]. Recently, Irfan and Shah [24], solved the time fractional telegraph equation with DBC using Fibonacci wavelet method. Shah [23] used the wavelet collocation technique to solve Bioheat transfer model, additionally, they presented a computational wavelet-based approach for tackling the dual-phase-lag system of bioheat transfer under hyperthermia [12]. P. Yadav et al. [31], solved the Fredholm integral equations of second kind using Fibonacci wavelet collocation method. Motivated by the advantages of Haar wavelets over other wavelets and their appealing features, we are deeply inspired to solve hyperbolic telegraph equation (1.1) by operational matrices of integration of Haar wavelet technique. The operational matrix approximation converts the main problem into simple algebraic equations whose solutions can be obtained using Newton's method. The benefits of the suggested method over previously published methods are as follows:

- This method unlike standard methods, does not entail the calculation of the Haar matrix's inverse.
- The primary chunks of Haar wavelet operational matrices are generated once and reused in for further computations, the CPU time is significantly reduced.
- Direct and simple applicability, with no need for intermediate approaches. The proposed method avoids the occurrence of numerical instability.
- This technique is highly practical for resolving boundary value problems, because these conditions are instantly considered.

Article is organized as: A brief description of the Haar wavelet and operational matrices of integration is discussed in section 2. In section 3, the description of solution technique for telegraph equations is provided. Section 4, present some numerical examples to emphasize the efficiency and precision of the prescribed numerical technique, and in section 5 conclusion is drawn.

2. HAAR WAVELET AND OPERATIONAL MATRICES

Here, our focus is to develop operational matrices for Haar wavelets. Since Haar wavelet is the oldest and simplest kind of orthonormal wavelet with a compact support. Alfred Haar [10] a Hungarian mathematician, proposed the Haar wavelet in 1910.

Haar wavelet [16]: The Haar wavelet is a series of weighted square-shaped functions that together constitute a wavelet basis. The mother wavelet for $z \in [0, 1)$, is defined as:

$$(2.1) \quad h_i(z) = \begin{cases} 1 & z \in [\alpha, \beta), \\ -1 & z \in [\beta, \gamma), \\ 0 & \text{otherwise.} \end{cases}$$

Where $\alpha = \frac{k}{2^j}$, $\beta = \frac{k+0.5}{2^j}$, $\gamma = \frac{k+1}{2^j}$, here $j = 0, 1, \dots, m-1$, $m = 2^{j+1}$, and $j = 0, 1, \dots, M$, indicates the maximum level of resolution. Also $i = k + 2^j - 1$, $0 \leq j < i$, and $1 \leq k < 2^{j+1}$, $j, k \in \mathbb{Z}$, are decomposition of index i . For $i = 0$, we have the scaling function for Haar wavelet family (1.1).

$$(2.2) \quad h_0(z) = \begin{cases} 1 & z \in [0, 1), \\ 0 & \text{otherwise.} \end{cases}$$

A function $\rho(z) \in L^2[0, 1]$, can be decomposed as an infinite series of functions that is

$$\rho(z) = \sum_{i=1}^{\infty} c_i h_i(z).$$

This series is truncated to a limited number of terms in a bid to approximate by utilizing Haar wavelet. Thus, any $\rho(z) \in L^2[0, 1]$, can be interpreted as.

$$\rho(z) \cong \sum_{i=1}^N c_i h_i(z), \quad N = 2^{j+1},$$

where j indicate highest degree of resolution. Following collocation points are considered to discretize Haar functions $h_i(z)$ by dividing the interval

$$z_l = \frac{l - 0.5}{N}, \quad l = 1, 2, \dots, N.$$

Operational Matrices of Integration: In order to construct the operational matrices of integration via Haar wavelet we integrate (2.1) as:

$$P_{i,1}(z) = \int_0^z h_i(z') dz',$$

and

$$P_{i,2}(z) = \int_0^z P_{i,1}(z') dz'.$$

These integrals can be calculated by using equation (1.1) as follows:

$$P_{i,1}(z) = \begin{cases} z - \alpha & z \in (\alpha, \beta), \\ \gamma - z & z \in [\beta, \gamma), \\ 0 & \text{otherwise.} \end{cases}$$

And $P_{i,2}(z)$ as follows

$$P_{i,2}(z) = \begin{cases} \frac{(z-\alpha)^2}{2} & z \in [\alpha, \beta), \\ \frac{1}{4m^2} - \frac{(\gamma-z)^2}{2} & z \in [\beta, \gamma), \\ \frac{1}{4m^2} & z \in [\gamma, 1), \\ 0 & \text{otherwise.} \end{cases}$$

For illustration $j = 2$, implies $N = 8$, we obtain Haar coefficient matrix H with dimension $N \times N$

$$H = \begin{bmatrix} 1 & 1 & 1 & 1 & 1 & 1 & 1 & 1 \\ 1 & 1 & 1 & 1 & -1 & -1 & -1 & -1 \\ 1 & 1 & -1 & -1 & 0 & 0 & 0 & 0 \\ 0 & 0 & 0 & 0 & 1 & 1 & -1 & -1 \\ 1 & -1 & 0 & 0 & 0 & 0 & 0 & 0 \\ 0 & 0 & 1 & -1 & 0 & 0 & 0 & 0 \\ 0 & 0 & 0 & 0 & 1 & 1 & 0 & 0 \\ 0 & 0 & 0 & 0 & 0 & 0 & 1 & -1 \end{bmatrix}$$

The operational matrices of integration P_1 and P_2 for collocation points z_l , is given by

$$P_1 = \begin{bmatrix} 0.0625 & 0.1875 & 0.3125 & 0.4375 & 0.5625 & 0.6875 & 0.8125 & 0.9375 \\ 0.0625 & 0.1875 & 0.3125 & 0.4375 & 0.4375 & 0.3125 & 0.1875 & 0.0625 \\ 0.0625 & 0.1875 & 0.1875 & 0.0625 & 0 & 0 & 0 & 0 \\ 0 & 0 & 0 & 0 & 0.0625 & 0.1875 & 0.1875 & 0.0625 \\ 0.0625 & 0.0625 & 0 & 0 & 0 & 0 & 0 & 0 \\ 0 & 0 & 0.0625 & 0.0625 & 0 & 0 & 0 & 0 \\ 0 & 0 & 0 & 0 & 0.0625 & 0.0625 & 0 & 0 \\ 0 & 0 & 0 & 0 & 0 & 0 & 0.0625 & 0.0625 \end{bmatrix}$$

$$P_2 = \begin{bmatrix} 0.0020 & 0.0176 & 0.0488 & 0.0957 & 0.1582 & 0.2363 & 0.3301 & 0.4395 \\ 0.0020 & 0.0176 & 0.0488 & 0.0957 & 0.1543 & 0.2012 & 0.2324 & 0.2480 \\ 0.0020 & 0.0176 & 0.0449 & 0.0605 & 0.0625 & 0.0625 & 0.0625 & 0.0625 \\ 0 & 0 & 0 & 0 & 0.0020 & 0.0176 & 0.0449 & 0.0605 \\ 0.0020 & 0.0137 & 0.0156 & 0.0156 & 0.0156 & 0.0156 & 0.0156 & 0.0156 \\ 0 & 0 & 0.0020 & 0.0137 & 0.0156 & 0.0156 & 0.0156 & 0.0156 \\ 0 & 0 & 0 & 0 & 0.0020 & 0.0137 & 0.0156 & 0.0156 \\ 0 & 0 & 0 & 0 & 0 & 0 & 0.0020 & 0.0137 \end{bmatrix}$$

3. DESCRIPTION OF METHOD

Consider second order PDEs with initial and boundary conditions

$$(3.1) \quad \frac{\partial^2 \rho(z, t)}{\partial t^2} + 2a \frac{\partial \rho(z, t)}{\partial t} + b^2 \rho(z, t) = \frac{\partial^2 \rho(z, t)}{\partial z^2} + R(z, t), \quad 0 \leq z \leq 1, \quad t \geq 0.$$

With ICs

$$\rho(z, 0) = f(z), \quad \frac{\partial \rho(z, 0)}{\partial \rho} = f_1(z), \quad 0 \leq z \leq 1.$$

DBC's

$$\rho(0, t) = \Theta_0(t), \quad \rho(1, t) = \Theta_1(t), \quad 0 \leq t \leq 1,$$

and NBC's

$$\frac{\partial \rho(0, t)}{\partial z} = \Theta_0(z), \quad \frac{\partial \rho(z, 0)}{\partial t} = \Theta_1(z).$$

Now expand $\ddot{\rho}$ in term of Haar wavelets we have

$$(3.2) \quad \ddot{\rho}''(z, t) = \sum_{i=1}^N c_i h_i(z),$$

where c_i , $i = 1, 2, 3, \dots, N$ is the coefficient of Haar to be calculated and “.” and “.” represent differentiation with regard to t and z respectively. Integrate equation (3.2) with regard to t and z , we obtain

$$(3.3) \quad \dot{\rho}''(z, t) = \Delta t \sum_{i=1}^N c_i h_i(z) + \dot{\rho}''(z, t_n),$$

where $\Delta t = t - t_n$

$$(3.4) \quad \rho''(z, t) = \frac{1}{2} \Delta^2 t \sum_{i=1}^N c_i h_i(t) + \Delta t \dot{\rho}' \rho(z, t_n) + \rho''(z, t_n),$$

(3.5)

$$\rho'(z, t) = \frac{1}{2} \Delta^2 t \sum_{i=1}^N c_i P_{i,1}(t) + \Delta t [\dot{\rho}'(z, t_n) + \dot{\rho}'(0, t_n)] + \rho'(z, t_n) - \rho'(0, t_n) + \rho'(0, t),$$

$$(3.6) \quad \rho(z, t) = \frac{1}{2} \Delta^2 t \sum_{i=1}^N c_i P_{i,2}(z) + \Delta t [\dot{\rho}(z, t_n) - \dot{\rho}(0, t_n) - z \dot{\rho}'(0, t_n)] +$$

$$\rho(z, t_n) - \rho(0, t_n) - z [\rho'(0, t_n) - \rho'(0, t)] + \rho(0, t),$$

$$(3.7) \quad \dot{\rho}(z, t) = \frac{1}{2} \Delta t \sum_{i=1}^N c_i P_{i,2}(z) + [\dot{\rho}(z, t_n) - \dot{\rho}(0, t_n) - z \dot{\rho}'(0, t_n)] + z \dot{\rho}'(0, t) - \dot{\rho}(0, t),$$

$$(3.8) \quad \ddot{\rho}(z, t) = \sum_{i=1}^N c_i P_{i,2}(z) + z \ddot{\rho}'(0, t) + \ddot{\rho}(0, t).$$

Plug $x = 1$ in the equation (3.6) and (3.8) to utilize the initial and boundary condition, then we obtain

$$(3.9) \quad \rho'(0, t) - \rho'(0, t_n) = -\frac{1}{2}\Delta^2 t \sum_{i=1}^N c_i P_{i,2}(1) - \Delta t [\Theta'_1(t_n) - \Theta'_0(t_n) - \dot{\rho}'(0, t_n)] + \Theta_1(t) - \Theta_1(t_n) + \Theta_0(t_n) - \Theta_0(t).$$

$$(3.10) \quad \dot{\rho}'(0, t) = -\sum_{i=1}^N c_i P_{i,2}(1) - \Theta''_0(t) + \Theta''_1(t).$$

Substitute (3.9) and (3.10) into the equation (3.4) and (3.6) and discretize, the result by assuming $z \rightarrow z_l$ and $t \rightarrow t_{n+1}$, we compute

$$(3.11) \quad \rho''(z_l, t_{n+1}) = \frac{1}{2}\Delta^2 t \sum_{i=1}^N c_i h_i(z_l) + \Delta t \dot{\rho}''(z_l, t_n) + \rho''(z_l, t_n).$$

$$(3.12) \quad \rho'(z_l, t_{n+1}) = \frac{1}{2}\Delta^2 t \sum_{i=1}^N c_i P_{i,1}(z_l) + \Delta t \dot{\rho}'(z_l, t_n) + \rho'(z_l, t_n) - \frac{1}{2}\Delta^2 t \sum_{i=1}^N c_i P_{i,2}(1) - \Delta t [\Theta'_1(t_n) - \Theta'_0(t_n)] + \Theta'_1(t_{n+1}) - \Theta'_1(t_n) + \Theta'_0(t_n) + \Theta'_0(t_n).$$

$$(3.13) \quad \rho(z_l, t_{n+1}) = \frac{1}{2}\Delta^2 t \sum_{i=1}^N c_i P_{i,1}(z_l) + \Delta t [\dot{\rho}(z_l, t_n) + \dot{\rho}(z_l, t_n)] + \rho(z_l, t_n) - \rho(0, t_n) - \frac{z_l}{2}\Delta^2 t \sum_{i=1}^N c_i P_{i,2}(1) - z_l \Delta t [\Theta'_1(t_n) - \Theta'_0(t_n)] - z_l [\Theta_1(t_n) - \Theta_0(t_n) + \Theta_0(t_{n+1}) - \Theta_1(t_{n+1})] + \Theta'_0(t_{n+1}).$$

$$(3.14) \quad \dot{\rho}(z_l, t_{n+1}) = \Delta t \sum_{i=1}^N c_i P_{i,1}(z_l) + [\dot{\rho}(z_l, t_n) + \dot{\rho}(0, t_n)] + z_l \Delta t \sum_{i=1}^N c_i P_{i,2}(1) - z_l [\Theta'_1(t_n) - \Theta'_0(t_n)] - z_l [\Theta'_0(t_{n+1}) - \Theta'_1(t_{n+1})] + \Theta'_0(t_{n+1}),$$

where

$$P_{i,2}(1) = \begin{cases} 0.5 & \text{if } i = 1 \\ \frac{1}{4m^2} & \text{if } i > 1. \end{cases}$$

$$(3.15) \quad \ddot{\rho}(z_l, t_{n+1}) = \Delta t \sum_{i=1}^N c_i [P_{i,1}(z_l) - z_l P_{i,1}(1)] - z_l [\Theta_0''(t_{n+1}) - \Theta_1'(t_{n+1})] - \Theta_0'(t_{n+1}).$$

After substituting (3.15) (3.14) and (3.11) in (1.1) we have,

$$(3.16) \quad \begin{aligned} & \Delta t \sum_{i=1}^N c_i [P_{i,1}(z_l) - z_l P_{i,1}(1)] - z_l [\Theta_0''(t_{n+1}) - \Theta_1'(t_{n+1})] - \Theta_0'(t_{n+1}) \\ & + 2[\Delta t \sum_{i=1}^N c_i P_{i,1}(z_l) + [\dot{\rho}(z_l, t_n) + \dot{\rho}(0, t_n)]] + z_l \Delta t \sum_{i=1}^N c_i P_{i,2}(1) - \\ & z_l [\Theta_1'(t_n) - \Theta_0'(t_n)] - z_l [\Theta_0'(t_{n+1}) - \Theta_1'(t_{n+1})] + \Theta_0'(t_{n+1})] + b^2 \rho(z, t) = \\ & \frac{1}{2} \Delta^2 t \sum_{i=1}^N c_i h_i(z_l) + \Delta t \dot{\rho}''(z_l, t_n) + \rho''(z_l, t_n). \end{aligned}$$

This is an algebraic equation system, resolving it using Newton's methods we find the Haar wavelet coefficient c_i after substituting these coefficient in (3.13) we get the approximate solutions.

4. APPLICATIONS AND RESULTS

Here, the telegraph equation of the form (1.1) is solved via the Haar wavelet collocation approach. For the purpose of demonstrating the efficacy of the suggested numerical technique, we have taken into account a few edge cases on (1.1). These are the examples that are being considered since either the exact solution has been found for them or they are solved in a similar fashion utilising other numerical methods. The precision of the Haar wavelet collocation methods is computed by the absolute error L_2 and maximum absolute errors L_∞ by using the formulas given as:

$$L_2 = \|\rho(z, t) - \rho_{n,m}(z, t)\|,$$

$$L_\infty = \max |\rho(z, t) - \rho_{n,m}(z, t)|,$$

where $\rho(z, t)$ and $\rho_{n,m}(z, t)$ are precise and approximate solutions respectively. Whole computational work is done on (Matlab–R2022a). To test the accuracy and convergence of solutions for one-dimensional problems, we utilized the following theorem of convergence, for the proof one can see [25].

Theorem 4.1. Let $f \in L^2(R)$ be a continuous function defined on $[0, 1)$ whose first derivative is bounded, then the error norm at the j -th level satisfies the following inequality

$$\|Em\| = \|u(x) - u_m(x)\| \leq \frac{K^2}{12} \left(\frac{1}{2M} \right)^2,$$

where $K > 0$ and M is a positive number related to the resolution level j -th of the wavelet by $M = 2^j$.

Example 4.1. Consider the case when $a = 6$, $b = 2$, $0 \leq x \leq 1$ we have telegraph equation (1.1) as

$$(4.1) \quad \frac{\partial^2 \rho(z, t)}{\partial t^2} + 12 \frac{\partial \rho(z, t)}{\partial t} + 4\rho(z, t) = \frac{\partial^2 \rho(z, t)}{\partial z^2} + R(z, t), \quad 0 \leq z \leq 1, \quad t \geq 0.$$

with ICs $\rho(z, 0) = \sin(z)$, $\frac{\partial \rho(z, 0)}{\partial t} = 0$, $0 \leq z \leq 1$, DBCs

$$\rho(0, t) = 0, \quad \rho(1, t) = \cos(t) \sin(1), \quad 0 \leq t \leq 1,$$

$$R(z, t) = -12 \sin(t) \sin(z) + 4 \cos(t) \sin(z).$$

The precise solution is $\rho(z, t) = \cos(t) \sin(z)$. After solving with Haar wavelet collocation technique we obtain the following system of algebraic equation:

$$(4.2) \quad \sum_{i=1}^N c_i [P_{i,2}(z_l) - z_l P_{i,2}(1) + 12\Delta t P_{i,2}(z_l) - 12\Delta t P_{i,2}(1) - 2z_l \Delta^2 t P_{i,2}(1) + 2z_l \Delta^2 t P_{i,2}(z_l)] =$$

$$\Delta t \sin(t_{n+1}) \sin(z_l) - \cos(z_{n+1}) \sin(z_l) - 12x_l \sin(t_n) \sin(z_l) - 12 \sin(t_{n+1}) \sin(z_l) +$$

$$12 \sin(t_{n+1}) \sin(1) + 4[\cos(t_{n+1}) \sin(z_l) - \cos(t_n) \sin(z_l)] - 4z_l [\Delta t \sin(t_n) \sin(1) -$$

$$\cos(t_n) \sin(1)] - \cos(t_n) \sin(1) + x_l \cos(t_{n+1}) \sin(1).$$

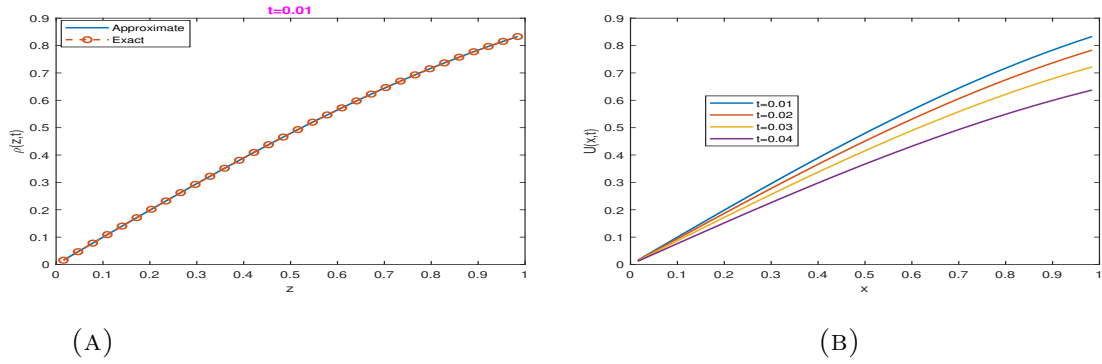


FIGURE 1. (A) At $j = 4$, comparison of approximate and exact solution of example 4.1 (B) Behaviour of approximate solutions at different time levels.

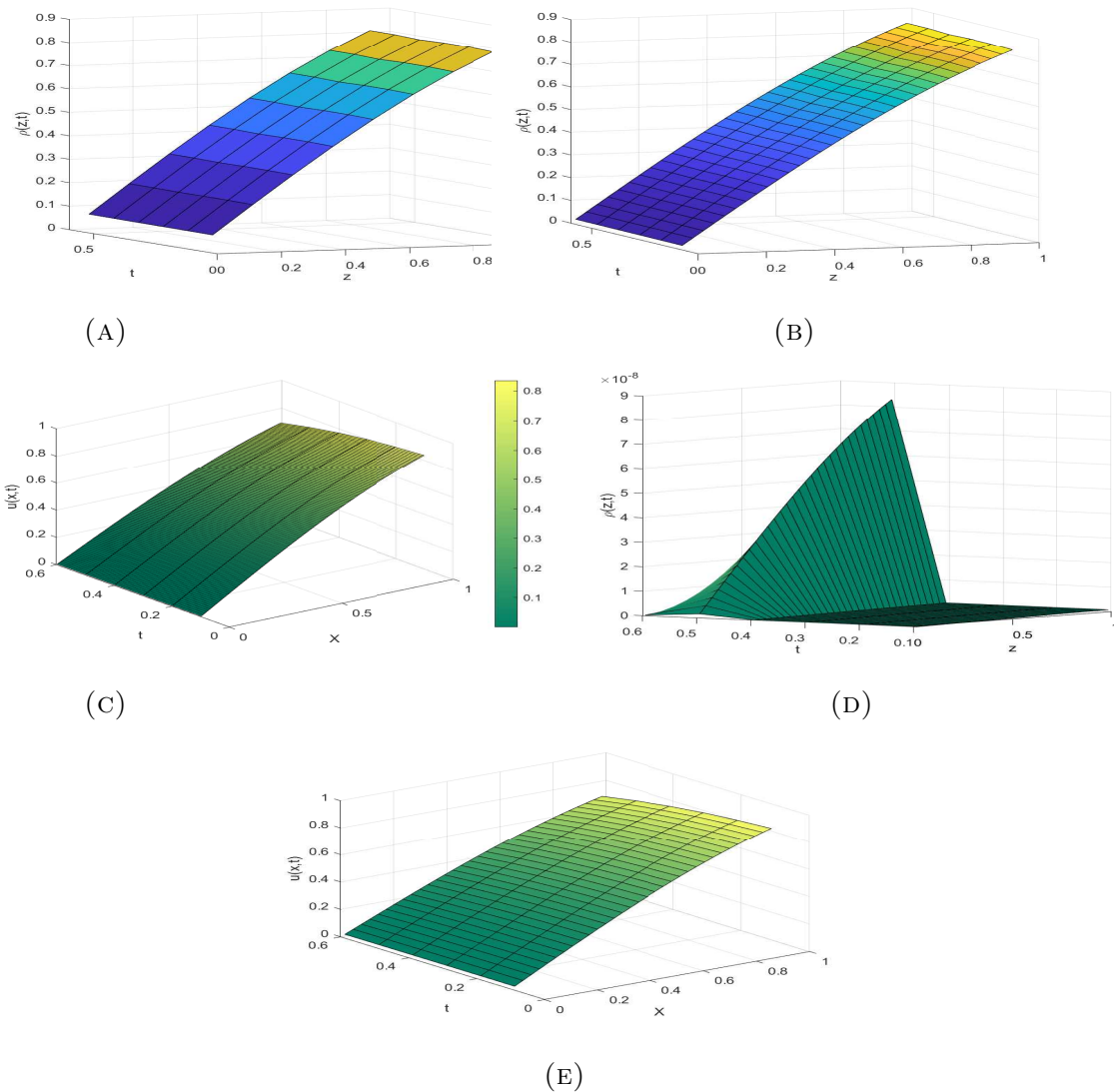


FIGURE 2. (A), (B),(C) behaviour of approximate solutions at different resolutions. (D) Shows the absolute error (E) exact solution.

TABLE 1. L_∞ at various t values are compared, of example 4.1.

$time(t)$	Present Method	MWGM [13]	CUBSM [18]	CUBTSM [21]
0.01	4.53e-12	5.70e-10	5.24e-06	4.63e-06
0.02	1.81e-12	3.83e-10	8.61e-06	1.01e-05
0.04	2.72e-12	3.84e-10	1.25e-05	1.42e-05
0.06	3.62e-11	5.74e-10	2.03e-05	1.71e-05
0.08	1.06e-11	1.46e-10	2.75e-05	1.90e-05

TABLE 2. Effects of time parameter t and the resolution level j , of example 4.1.

Resolution level j	Error	t=0.01	t=0.03	t=0.05	t=0.07
3	L_∞	8.241e-05	7.417e-06	2.060e-05	3.215e-05
	L_2	1.556e-05	2.812e-06	9.887e-06	4.081e-05
4	L_∞	8.329e-05	7.496e-05	2.082e-05	2.582e-05
	L_2	1.091e-06	1.713e-05	1.171e-06	3.582e-06
6	L_∞	8.393e-06	7.554e-06	2.098e-05	4.120e-05
	L_2	3.906e-06	5.712e-06	3.857e-06	3.121e-06

To find the Haar coefficients c_i solve the system of algebraic equation with Newton's method, using these Haar coefficient in (3.13) we have the approximate solutions. In Table 1, we compares L_∞ for different values of t , enabling one to analyze the efficacy and accuracy of the proposed technique. Clearly, the results obtained by using Haar wavelet are highly efficient in comparison to multi-wavelet Galerkin method [13] and cubic B-splines method [21]. In Table 2, the effects of the time parameters t for different resolution levels $j = 2, 4, 6$ are presented. As we increase the resolution levels the error decreases exponentially and results are more accurate.

Example 4.2. Consider the case when $a = 0.5$, $b = 1$, $0 \leq z \leq 1$ as

$$(4.3) \quad \frac{\partial^2 \rho(z, t)}{\partial t^2} + \frac{\partial \rho(z, t)}{\partial t} + \rho(z, t) = \frac{\partial^2 \rho(z, t)}{\partial z^2} + R(z, t), \quad 0 \leq z \leq 1, \quad t \geq 0.$$

With ICs $\rho(z, 0) = \sin(z)$, $\frac{\partial \rho(z, 0)}{\partial t} = 0$, $0 \leq z \leq 1$.

DBC's $\rho(0, t) = 0$, $\rho(1, t) = 0$, $0 \leq t \leq 1$. $R(z, t) = (2 - 2t + t^2)(z - z^2)e^{-t} + 2t^2e^{-t}$.

Exact solution of (4.3) is $\rho(z, t) = (z - z^2)t^2e^{-t}$.

Now solving this problem using Haar wavelet method we have

$$(4.4) \quad \sum_{i=1}^N c_i [P_{i,2}(z_i) - z_i P_{i,2}(1) + \Delta t P_{i,2}(z_i) - z_i \Delta t P_{i,2}(1)] = 2t^2e^{-t} - (z - z^2)t^2e^{-t} + (2 - 2t + t^2)(z - z^2)e^{-t} + 2t^2e^{-t} + (z - z^2)e^{-t} + 2t - \Delta t(2e^{-t}2t + 2e^{-t}t^2) - 2(2 - 2t + t^2)e^{-t}.$$

Equation (4.4) is the system of algebraic equation for example 4.2, which on solving by Newton's method, coefficient c_i s are calculated. By using these coefficient in (3.13) we obtain the approximate solutions.

TABLE 3. Maximum absolute error (L_∞) at various t values are compared, of example 4.2.

$time(t)$	Present method	CUBSM [18]	CUBTSM [21]
0.01	2.177e-12	8.76e-05	5.91e-05
0.03	1.687e-12	3.29e- 05	1.78e-05
0.05	1.607e-12	5.90e-06	1.43e- 05
0.07	1.527e-12	3.04e-05	1.35e-05
0.09	2.153e-11	6.92e-06	5.20e-06

TABLE 4. Effects of time parameter t and the resolution level $N = 2^{j+1}$, of example 4.2.

j	Error	$t=0.01$	$t=0.03$	$t=0.05$	$t=0.07$
3	L_∞	2.177e-12	1.687e-12	1.607e-12	1.527e-12
	L_2	2.692e-13	2.692e-13	1.446e-13	4.647e-13
4	L_∞	2.142e-12	2.643e-12	1.946e-12	1.853e-12
	L_2	4.925e-14	4.695e-14	4.521e-14	4.315e-14
6	L_∞	2.758e-13	2.758e-13	2.628e-13	2.312e-13
	L_2	1.292e-14	4.181e-14	8.599e-14	6.658e-14

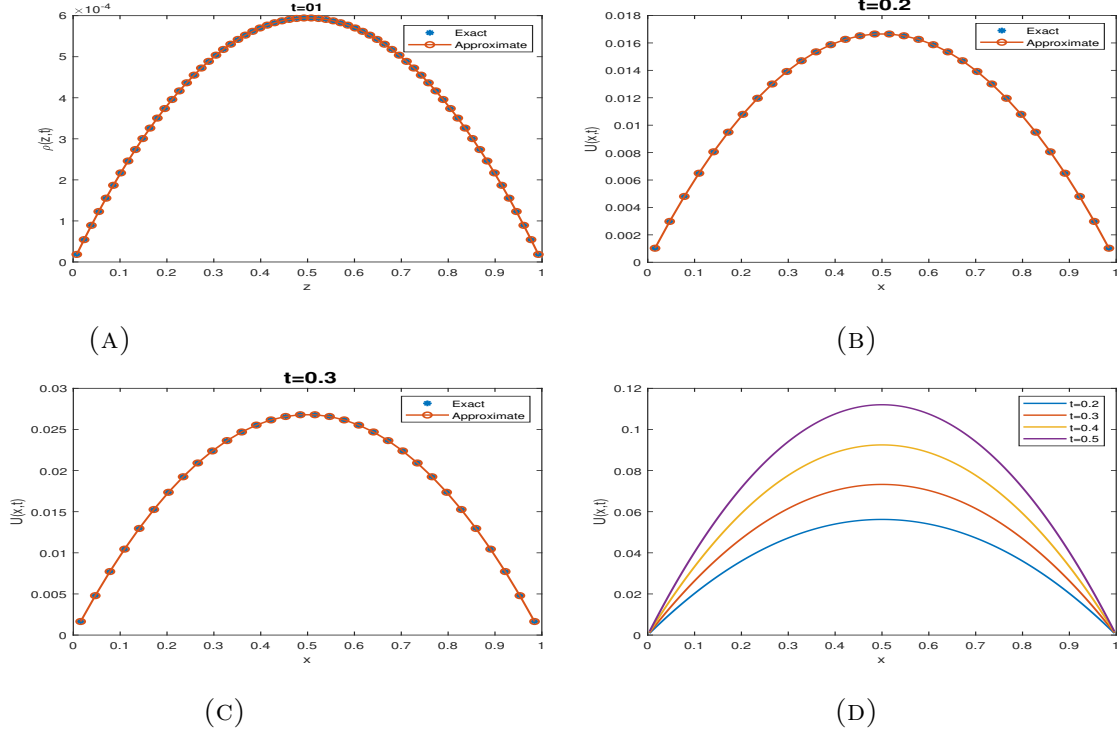


FIGURE 3. (A), (B) and (C) shows the comparison of exact and Haar solution at $t = 0.1$, $t = 0.2$ $t = 0.3$ and the resolution $j = 4$. (D) shows approximate solution at various time levels.

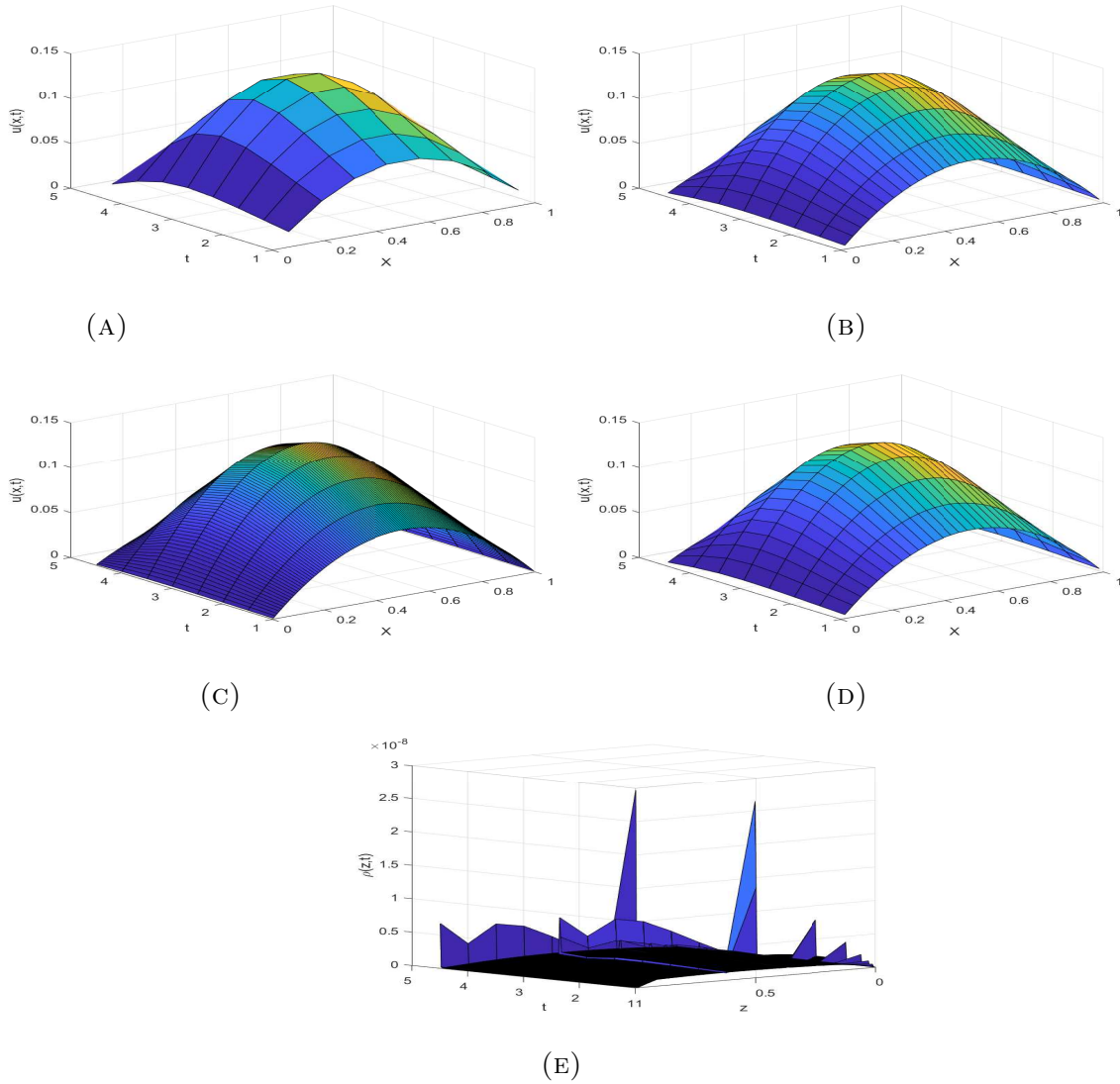


FIGURE 4. Physical behaviour of numerical solution is shown at different resolution level i.e. $N = 2^{j+1}$ (A) at $j = 2$ (B) at $j = 4$ (C) at $j = 6$ (D) shows physical behaviour of exact solution at $j = 4$ (E) Graphically depicts the behaviour of absolute error of example 4.2

Example 4.3. Consider equation (1.1) with $a = 0$, $b = 0$, $R(z, t) = 0$, and $a \leq z \leq b$ as

$$(4.5) \quad \frac{\partial^2 \rho(z, t)}{\partial t^2} + \frac{\partial \rho(z, t)}{\partial t} + \rho(z, t) = \frac{\partial^2 \rho(z, t)}{\partial z^2} + R(z, t), \quad 0 \leq z \leq 1, \quad t \geq 0.$$

With ICs

$$\rho(z, 0) = z, \quad \frac{\partial \rho(z, 0)}{\partial \tau} = z^2, \quad 0 \leq z \leq 1.$$

NBCs

$$\frac{\partial u(0, t)}{\partial z} = 0, \quad \frac{\partial u(1, t)}{\partial z} = 1 + 2 \sinh(t), \quad 0 \leq t \leq 1.$$

Exact solution of (4.5) is

$$\rho(z, t) = z + z^2 \sinh(t).$$

By Haar wavelet collocation technique we obtain the system of algebraic equations as follows:

$$(4.6) \quad \sum_{i=1}^N c_i [P_{i,2}(z_l) - z_l P_{i,2}(1)] = \frac{z_l}{2} \rho''(z_l, t_n) + z_l \sinh(t_{n+1}).$$

Solved it using Newton's method or any other standard methods to find the Haar coefficient c_i using these coefficient in (3.13) we obtain the approximate solutions.

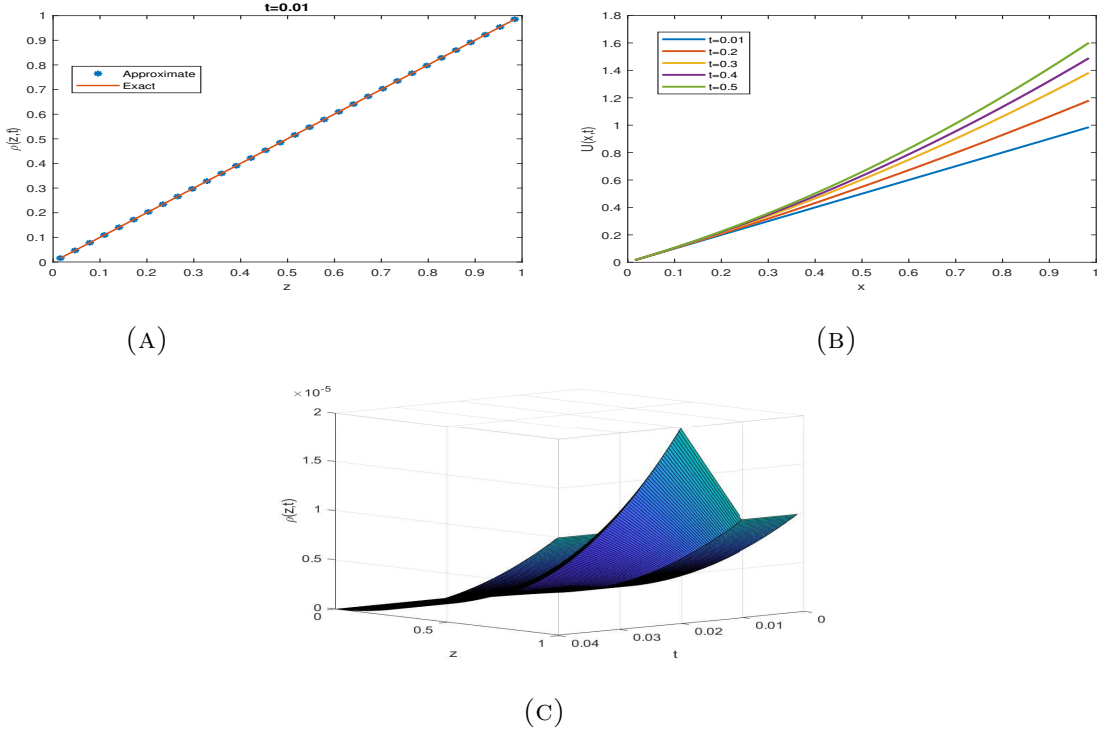


FIGURE 5. (A) Representation of approximate solution and exact solution at $j=4$ (B) Approximate solution at various time levels (C) Represents the behaviour of absolute error at resolution $j = 5$

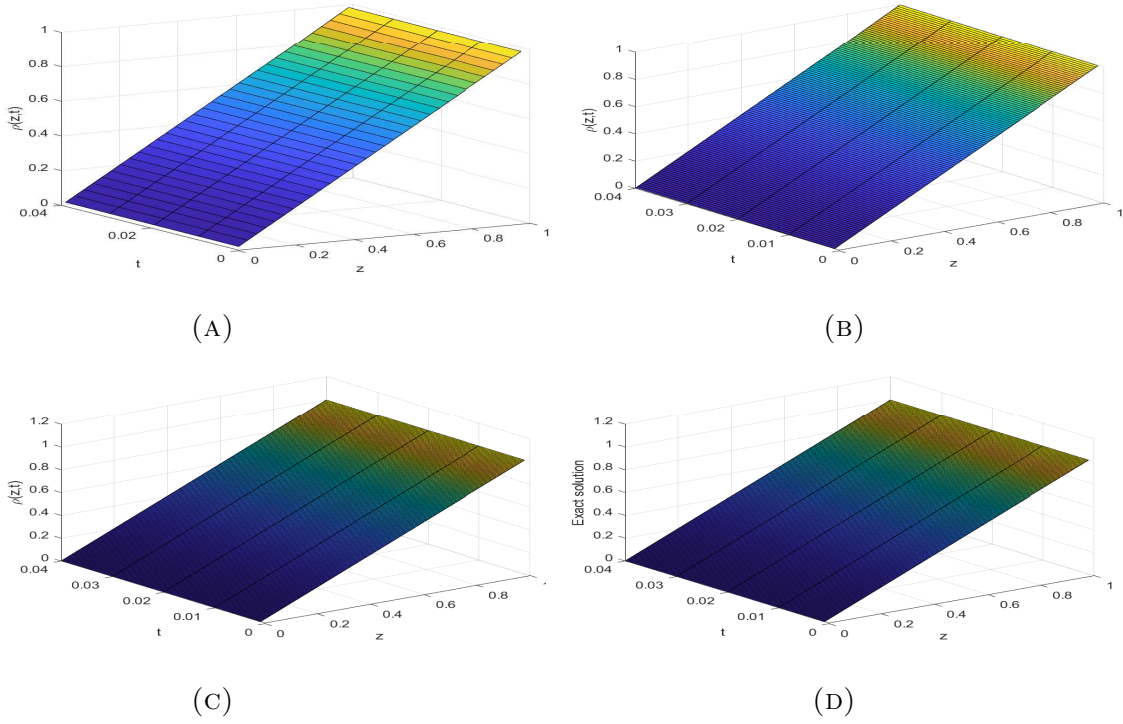


FIGURE 6. (A),(B),(C) 3D representation of numerical solution at resolution level $j = 4, 6, 7$ (D) exact solution at $j = 7$.

TABLE 5. Absolute error at various t values, for a fixed resolution level $j = 4$, of example 4.3.

collocation point	t=0.01	t=0.03	t=0.05
0.1	2.4415e-08	9.7703e-07	1.0964e-06
0.2	6.1045e-07	8.7902e-06	2.0121e-06
0.3	6.0743e-06	1.2258e-06	2.9163e-05
0.4	1.4067e-06	1.2258e-05	3.2352e-05
0.5	2.4447e-05	1.2519e-05	3.2536e-04
0.6	1.3555e-05	1.1639e-05	3.0622e-04
0.7	1.1468e-05	9.6966e-04	2.2539e-04
0.8	7.1498e-05	5.7511e-04	1.1249e-04
0.9	3.1206e-05	8.5397e-04	6.5703e-04

In Fig. 5,6 we present 3D graph of approximate and exact solutions at different resolution levels to demonstrate the efficiency of Haar wavelet collocation method the absolute error is calculated at different time and demonstrated it in the form of Table 5. The obtained results are compared with [13] and [21]. We see that the outcomes computed by Haar wavelet collocation method are quit efficient than other methods. The error decreases as the resolution levels increases and the approximate solutions is more closer to exact solution.

5. CONCLUSION

In this article, the hyperbolic telegraph equation with DBCs and NBCs are studied. The simplification was accomplished by constructing the operational matrices of integration of Haar wavelet. This method simplifies the problem to a sparse system of linear equations, which is then solved using Newton's method. The usability of the Haar wavelet collocation method is illustrated via three test examples with different boundary condition, we compare the obtained results with the multiwavelet Galerkin method [13], B-splines method [18] and cubic trigonometric B-spline method [21]. The obtained results demonstrates that the proposed technique for solving such problems is reliable and efficient. For higher number of collocation points, more precise results can be acquire, which is an essential features of the method. As we increase the resolution level the error decreases exponentially and the results are closer to exact solution. In examples 4.1, the maximum error is $1.81e - 12$, and in examples 4.2, at resolution $j = 6$ the maximum error is $1.292e - 14$. Also the error for $t = 0.01, 0.03, 0.05, 0.07$ corresponding to resolution levels $j = 3, 4, 6, 7$ is shown in Tables 2,4 and 5. The present approach can be applied to both BVPs and IVPs with a slight modification, but without the transformation of BVPs into IVPs or vice versa. Additionally, the method can easily be extended to solve physical and biological models.

Acknowledgement

We are highly thankful to Editor and the referees for giving the valuable comments and suggestions for the improvisation of the manuscript. The first author is supported

by UGC india and 3rd author is supported by Prince Sattam bin Abdulaziz University with project number (PSAU/2023/R/1444).

REFERENCES

[1] M. A. Abdou, Adomian decomposition method for solving the telegraph equation in charged particle transport, *J. Quant. Spectrosc. Radiat. Transf.*, 95 (2005), 407–414.

[2] A. O. Adewumi, S.O. Akindeinde, A. A. Aderogba, and B.S. Ogundare, Laplace transform collocation method for solving hyperbolic telegraph equation, *Int. J. of Eng. Math.*, 2017 (2017), 1-9.

[3] A. J. Acebrn, and A.M. Ribeiro, A Monte Carlo method for solving the one-dimensional telegraph equations with boundary conditions, *J. Comput. Phys.*, 305 (2016), 29–43.

[4] J. Benito, F. Urena, and L. Gavete, Solving parabolic and hyperbolic equations by the generalized finite difference method, *J. Comput. Appl. Math.*, 209 (2007), 208-233.

[5] J. Biazar, H. Ebrahimi, and Z. Ayati, An approximation to the solution of telegraph equation by variational iteration method, *Numer. Methods Partial Differ. Equ.*, 25 (2009), 797-801.

[6] C. F. Chen, and C.Hsiao, Haar wavelet method for solving lumped and distributed-parameter systems, *IEE Proc-Control Theory and Applications*, 144 (1997), 87–94.

[7] M. Dehghan and A. Ghesmati, Solution of the second-order one-dimensional hyperbolic telegraph equation by using the dual reciprocity boundary integral equation (DRBIE) method, *Eng. Anal. Bound. Elem.*, 34 (2010), 51–59.

[8] G. Hariharan, and K. Kannan, and K. R. Sharma. Haar wavelet method for solving Fisher’s equation, *Applied Math. and comput.*, 211 (2009), 284-292.

[9] G. Hariharan, and K. Kannan, Haar wavelet method for solving FitzHugh-Nagumo equation, *Intl. J. Math. Stat. Science.*, 2(2010).

[10] A. Haar, Zur Theorie der orthogonalen Funktionensysteme, (German) *Math. Ann.*, 69 (1910), 331–371.

[11] B. Hussain, Afroz and Shah Jahan, Approximate solution for proportional-delay Riccati differential equations by Haar wavelet method, *Poincare J. Anal. Appl.*, 8, no. 2 (2021), 155-168.

[12] M. Irfan, and F. A. Shah, Numerical Solution of Bioheat Transfer Model using Generalized Wavelet Collocation Method, *Jordan J. Math. Stat.*, 15 (2022), 211-229.

[13] H. B. Jebreen, Y. C. Cano, and I. Dassios, An efficient algorithm based on the multi-wavelet Galerkin method for telegraph equation, *AIMS Math.*, 6 (2021), 1296-1308.

[14] P. M. Jordan and A. Puri, Digital signal propagation in dispersive media, *J. Appl. Phys.*, 85 (1999), 1273-1282.

[15] U. Lepik, Numerical solution of evolution equations by the Haar wavelet method, *J. Appl. Math. Comput.* 185 (2007), 695–704.

- [16] U. Lepik, Numerical solution of differential equations using Haar wavelets, *Math. Comput. Simul.*, 68 (2005), 127–143.
- [17] U. Lepik, and H. Hein, Haar wavelets with applications, *Math. Eng. Springer.*, (2014).
- [18] R. C. Mittal and Bhatia, Numerical solution of second order one dimensional hyperbolic telegraph equation by cubic B-spline collocation method, *Appl. Math. Comput.*, 220 (2013), 496–506.
- [19] A. C. Metaxes and R. J. Meredith, Industrial microwave heating, *IET*. 4 (1993).
- [20] S. T. Mohyud-Din, and M. A. Noor and K. Inayat, Variational iteration method for solving telegraph equations, *Appl. Appl. Math.*, 4 (2009), 114–121.
- [21] T. Nazir, M. Abbas, and M. Yaseen, Numerical solution of second-order hyperbolic telegraph equation via new cubic trigonometric B-splines approach, *Cogent Math.*, 4 (2017), 1382061.
- [22] V. K. Srivastava, M. k. Awasthi, and R. K. Chaurasia, Reduced differential transform method to solve two and three dimensional second order hyperbolic telegraph equations, *J. King Saud Univ. Eng. Sci.*, 29 (2017), 166-171.
- [23] F. A. Shah and M. I. Awana, A computational wavelet method for solving dual-phase-lag model of bioheat transfer during hyperthermia treatment, *Comp. Math. Methods*, 2 (2020), e1095.
- [24] F. A. Shah, M. Irfan, K. S. Nisar, and R.T.Matoog, Fibonacci wavelet method for solving time-fractional telegraph equations with Dirichlet boundary conditions, *Results Phys.*, 24 (2021), 104123.
- [25] Siraj-ul-Islam, I. Aziz and B. Sarler, The numerical solution of second-order boundary-value problems by collocation method with the Haar wavelets, *Math. Comput. Model.*, 52 (2010), 1577–1590.
- [26] Siraj-ul-Islam, I. Aziz and B. Sarler, Wavelets collocation methods for the numerical solution of elliptic BV problems, *Appl. Math. Model.* 37 (2013), 676–694.
- [27] V. H. Weston, and S. Wave, splitting of the telegraph equation in \mathbf{R}^3 and its application to inverse scattering, *Inverse Probl.*, 9 (1993), 789–812.
- [28] A. Yildirim, homotopy perturbation method for solving the space-and time-fractional telegraph equations, *Int. J. Comput. Math.*, 87(2010), 2998–3006.
- [29] P. Yadav, Shah Jahan, and K.S. Nisar, Solving fractional Bagley-Torvik equation by fractional order Fibonacci wavelet arising in fluid mechanics., *Ain Shams Eng. J.*, (2023), 102299.
- [30] S. A. Yousefi, Legendre multiwavelet Galerkin method for solving the hyperbolic telegraph equation, *Numer. Methods Partial Differ. Equ.*, 26 (2010), 535–543.
- [31] P. Yadav, S. Jahan, and K.S. Nisar, Fibonacci Wavelet Collocation Method for Fredholm Integral Equations of Second Kind, *Qual. Theory. Dyn. Syst*, 22, 82 (2023).

(1) DEPARTMENT OF MATHEMATICS,CENTRAL UNIVERSITY OF HARYANA, MAHENDERGARH-123029, INDIA

Email address: `shahid201344@cuh.ac.in`

(2) DEPARTMENT OF MATHEMATICS,CENTRAL UNIVERSITY OF HARYANA, MAHENDERGARH-123029, INDIA

Email address: `Shahjahan@cuh.ac.in`

(3) DEPARTMENT OF MATHEMATICS, COLLEGE OF SCIENCE AND HUMANITIES IN ALKHARJ, PRIENCE SATTAM BIN ABDULAZIZ UNIVERSITY ALKHARJ 11942, SAUDI ARABIA

Email address: `n.sooppy@psau.edu.sa`